Available online at www.sciencedirect.com
ScienceDirect
Catalysis Today 133–135 (2008) 154–159
CATALYSIS TODAY
www.elsevier.com/locate/cattod

One pot preparation of NiO/ZrO_2 sulfated catalysts and its evaluation for the isobutene oligomerization

F.J. Tzompantzi [a], M.E. Manríquez [a], J.M. Padilla [a], G. Del Angel [a], R. Gómez [a,*], A. Mantilla [b]

[a] *Universidad Autónoma Metropolitana-Iztapalapa, Department of Chemistry, Av. San Rafael Atlixco No. 186, México 09340, D.F., Mexico*
[b] *CICATA, IPN, Av. Legaria 694, Col. Irrigación, México 11500, D.F., Mexico*

Available online 31 January 2008

Abstract

The synthesis of NiO/ZrO_2 sulfated catalysts prepared by the one pot method (sol–gel) is reported. Specific surface areas comprised between 52 and 108 m^2/g were obtained. XRD patterns showed the presence of monoclinic and tetragonal zirconia phases. FTIR-pyridine absorption spectra show the presence of Lewis and Brönsted sites in sulfated zirconia but only Lewis sites in nickel zirconia sulfated catalysts. A good correlation between the amount of adsorbed pyridine and the catalytic activity for the isopropanol dehydration was observed. However, an opposite effect was observed for the isobutene oligomerization, where the catalysts with the lower acidity showed the higher activity. The role of Ni^{+2} diminishing the deactivation rate forming π-allylic bonds with the olefins is discussed.

Keywords: Sulfated zirconia; Nickel zirconia sulfated catalysts; Olefins oligomerization; Isopropanol dehydration; Sol–gel zirconia catalysts; Pyridine adsorption on sulfated zirconia

1. Introduction

The oligomerization of butenes is a reaction with a wide range of important applications in the chemical and petrochemical industry, widely used in order to obtain branched $C_8^=$ or $C_{12}^=$ olefins; in the case of $C_8^=$ olefins, they are employed for the production of gasoline additives [1–4] and as the raw material for the plastic production industry in the case of $C_{12}^=$ olefins [5]. Industrially, the oligomerization is carried out by using a catalyst consisting in phosphoric acid supported in a solid [6]. Because of the nature of the catalyst used this process is considered highly pollutant. In addition, the process presents serious deactivation problems at the industrial operation conditions employed (140 °C and atmospheric pressure), caused firstly for the formation of $C_{16}^=$ olefins over the catalyst surface [7–10]. The absorbed $C_{16}^=$ olefins continue reacting in an uncontrolled polymerization reaction, until the formation of high molecular weight oligomers [11]. Therefore, one of the challenges in the oligomerization of butenes is the development of catalyst with high selectivity to the formation of the $C_8^=$–$C_{12}^=$ fractions, avoiding the formation of $C_{16}^=$ olefins or heavier fractions. In this way, there have been reported good results with catalyst of nickel supported in zeolites [12–14]. Sulfated alumina exchanged with nickel has been reported in a recent paper as an active and stable catalyst for the oligomerization of ethylene [15]. The authors propose the formation of Ni^{+1} as the active centers for this reaction.

Then, it is clear that to carry out the oligomerization reaction a catalyst with strong acidity is necessary, but at the same time with the capacity to control the size of the chain of the olefins obtained.

With this in mind, in the present work the results obtained in the oligomerization of isobutene over NiO/ZrO_2 sulfated catalysts are reported. The catalyst was prepared by the named ''one pot'' sol–gel procedure, starting from zirconium alkoxide and nickel sulfate.

2. Experimental

The synthesis of the catalysts was carried as follows; 30 ml bi-distilled water and 200 ml of ter-butanol were mixed in glass

* Corresponding author. Tel.: +52 55 58044668; fax: +52 55 5804466.
E-mail addresses: fjtz@xanum.uam.mx (F.J. Tzompantzi), gomr@xanum.uam.mx (R. Gómez), angelesmantilla@hotmail.com (A. Mantilla).

0920-5861/$ – see front matter © 2007 Elsevier B.V. All rights reserved.
doi:10.1016/j.cattod.2007.12.071

flak under constant stirring at 25 °C. Then, nickel sulfate ($NiSO_4$ $6H_2O$, J.T. Baker 99.7%) was added in appropriate amounts to get 3, 5 and 10 wt% of Ni in the catalysts, adjusting with nitric acid until reach a pH 3 in the solution. After that, 84.5 ml of zirconium *n*-butoxide (Aldrich 98%) were slowly added. This solution was put under reflux with constant stirring for 12 h. The catalysts were labeled as NiO/ZrO_2–SO_4–X, where X is the %wt Ni content. Sulfated zirconia without nickel was prepared following the same procedure used for NiO/ZrO_2 catalysts but instead of nitric acid, the pH of the gelling solution was adjusted to 3.0 with sulfuric acid. The catalyst was labeled as ZrO_2–SO_4. The obtained gels were dried at 100 °C for 12 h and then annealed in air at 600 °C for 12 h.

3. Characterization

3.1. Specific surface areas

The specific surface areas were determined by nitrogen adsorption with an Autosorb3 Multistation Quantachrome apparatus. First, the solids were treated at 350 °C under vacuum and then the nitrogen adsorption was carried out. The specific areas were calculated from the nitrogen volume adsorbed at 0.3 P/P_0 of relative pressure.

3.2. X-ray diffraction

The catalyst samples were characterized by X-ray diffraction (XRD), by using Cu Kα radiation, in Siemens D-500 equipment. The signal intensity was measured by step scanning in the 2θ range between 4 and 70 with a step of 0.03° and a measuring time of 2 s per point.

3.3. FTIR-pyridine adsorption

Lewis and Brönsted acid sites were determined by FTIR-pyridine adsorption with a Nicolet Nexus 479 FTIR spectrometer with a resolution of 3.8 cm^{-1} and 50 scans. The annealed material was passed into thin self-supported wafers. Then, they were placed in a glass Pyrex cell with CaF_2 windows coupled to a vacuum line, in order to be evacuated (1×10^{-6} Torr) in situ at 300 °C for 30 min. The adsorption was carried out on the cell at 25 °C by introducing to the cell the pyridine contained in a glass bulb coupled to the cell. The pyridine excess was desorbed in vacuum from room temperature to 400 °C, with 100 °C steps. The quantities of absorbed pyridine were obtained from the integrated absorbance of the respective bands.

3.4. Isopropanol dehydration

The isopropanol dehydration was carried out at atmospheric pressure and 130 °C over pre-activated catalysts (400 °C 2 h, in fluxed nitrogen). The isopropanol was fed by using a saturator system coupled to a fixed bed glass reactor (with a volume of 3 ml and using 20 mg of catalyst). The HGSV used for the isopropanol dehydration was 1 h^{-1}. The activity was followed by determining the isopropanol conversion and the selectivity was determined for propene and di-isopropyl ether (DIPE). The analysis of products was carried out with a gas chromatograph VARIAN CP-3800 coupled to the catalytic activity system and equipped with a capillary Quadrex Stationary phase, 007-FFAP with 30 m of length.

3.5. Isobutene oligomerization

The catalytic activity for the isobutene oligomerization reaction was determined using a fixed bed glass reactor (with a volume of 3 ml and using 200 mg of catalyst). The catalyst was activated at 400 °C in flowing nitrogen for 2 h, with a step of 1 ml/s. After the activation treatment, the temperature was lowered to 28 °C and then a mixture of isobutane/isobutene 50:50 (w/w) was fed into the reactor at atmospheric pressure, in order to assure that the hydrocarbon mixture was in gas phase. The GHSV value used for isobutene oligomerization was 16 h^{-1}.

The analysis of products was made with a FID gas chromatography (Shimadzu GC-8A) equipped with a 20% MBEA column of 24 ft, coupled to the reactant system. The conversion was calculated in function of isobutene converted and the selectivity is reported as $C_8^=$, $C_{12}^=$ and $C_{16}^=$ % mol fractions.

4. Results and discussion

4.1. Specific surface areas

The specific areas of the catalysts are reported in Table 1. It can be seen that the ZrO_2–SO_4 catalyst showed the highest area (130 m^2/g) in comparison with the catalysts containing Ni. The lowest value corresponds to the sample containing 10 wt% of Ni (59 m^2/g). The strong effect of Ni content in the diminution of the specific surface area is because the catalysts were prepared by co-gelling the zirconium alkoxide with nickel sulfate. Then, the insertion of nickel in the zirconia network could be expected and important modifications in the textural properties were induced.

Table 1
Nomenclature, textural, acidity properties and activity in the isopropanol dehydration of NiO/ZrO_2–SO_4 catalysts

Catalyst	Specific surface area (m^2/g)	Acidity (mmol py/m^2)	Propene[a] selectivity (%)	DIPE[a] selectivity (%)	Rate (mol/g s 10^6)[a]
ZrO_2–SO_4	130	0.43	87.4	12.5	4.1
Ni/ZrO_2–SO_4-3	77	0.48	85.0	14.9	1.1
Ni/ZrO_2–SO_4-5	108	0.39	81.5	18.4	0.9
Ni/ZrO_2–SO_4-10	59	0.86	74.8	25.2	0.4

[a] Determined from the isopropanol decomposition at 130 °C, atmospheric pressure and GHSV = 1 h^{-1}.

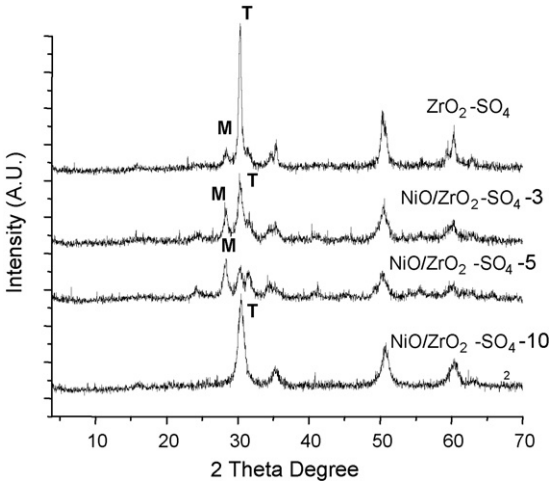

Fig. 1. X-ray diffraction spectra of the nickel zirconia sulfated catalysts annealed at 600 °C.

4.2. XRD spectra

XRD patterns of the different catalysts are showed in Fig. 1. Monoclinic and tetragonal zirconia crystalline phases were identified for ZrO_2–SO_4, NiO/ZrO_2-3 and NiO/ZrO_2-5; meanwhile, only tetragonal zirconia is observed in the NiO/ZrO_2-10 catalyst. We can say that a high nickel content confers a stabilization effect of the tetragonal crystalline phase. Additionally, it can also be observed that in the catalysts containing nickel, the XRD diffraction peaks identifying the tetragonal phase are broad: i.e. the crystallite size diminishes as the nickel content increases. Here, we study the effect of presence of nickel on the zirconia structural properties.

4.3. FTIR-pyridine adsorption

The pyridine thermodesorption spectra of the sulfated zirconia and nickel zirconia sulfated catalysts are presented in Fig. 2. For sulfated zirconia (a) we can observe the adsorption band at 1445 cm^{-1} assigned to pyridine coordinate in Lewis sites. The band at 1490 cm^{-1} is associated to Brönsted and Lewis sites and is due to the vibration of the pyridine ring. Another weak band is observed at 1545 cm^{-1}, associated with the presence of Brönsted acid sites. The band at 1575 cm^{-1} identifies weak Lewis acid sites and the band at 1600 cm^{-1} corresponds to strong Lewis acid sites [16]. Increasing the desorption temperature the intensity of the bands diminishes and finally at 400 °C practically no adsorption bands can be observed.

For the NiO/ZrO_2–SO_4 catalysts, the spectra of Fig. 2(b–d) showed the bands assigned to Lewis sites, which also diminishes with the desorption temperature; however, the band at 1545 cm^{-1} (corresponding to the Brönsted acid sites) is not present. The resistance to be desorbed in function of the temperature is considered as an indirect determination of the strength of the acid sites. The adsorption bands for the NiO/ZrO_2–SO_4 catalysts disappear at 300 °C in vacuum, which is a lower temperature than that observed in the ZrO_2–SO_4 (400 °C) catalyst. The results showed that the acidity of the reference catalyst is stronger than that obtained in the nickel zirconia sulfated catalysts.

On the other hand, the number of mmol of pyridine adsorbed was calculated from the intensity of the band at 1445 cm^{-1} (Lewis acid sites) in the desorption temperature of 200 °C and the calculated results are reported in Table 1 and expressed in mmol pyridine/m^2. The Lewis acidity in function of the specific surface (m^2) determined by the pyridine adsorption is almost of the same order in all the catalysts; however, the highest acid sites density corresponds to the catalyst with 10 wt% of Ni.

The nature of the acid sites on sulfated zirconia has been largely discussed and their suggested models have been a matter of several publications. For example, in Fig. 3 we report the modified models, illustrating the origin of the acidity in sulfated zirconia proposed by Ben Chaabene et al. [17].

4.4. Isopropanol dehydration

The isopropanol dehydration has been carried out in order to determine the acid properties of the catalysts. Several authors use this reaction as a reaction to measure the acid–base properties of various metal oxides [18,19]. In the isopropanol decomposition, the main product obtained is the olefin and the rate of dehydration is related the total acidity of the catalysts [20]. In Table 1, the activity and selectivity for the isopropanol dehydration is reported. The catalyst without nickel addition showed the highest activity. In NiO/ZrO_2–SO_4 catalysts an important diminution in the activity was observed. The rate goes down from 4.1 to 0.4×10^{-6} mol/g s for ZrO_2–SO_4 and NiO/ZrO_2–SO_4-10 catalysts, respectively. As higher is the reaction rate, higher is the acidity, corresponding then the following order to the total acidity of the catalysts:

$$ZrO_2-SO_4 > NiO/ZrO_2-SO_4\text{-}3 > NiO/ZrO_2-SO_4\text{-}5 > NiO/ZrO_2-SO_4\text{-}10$$

On the other hand, the selectivity patterns for the isopropanol dehydration give important information about the catalysts acidity. Propene and di-isopropyl ether are the principal products of the reaction. The formation of propene is related to the strength of the acid site, meanwhile the formation to di-isopropyl ether is almost a consequence of the acid sites density.

Recently, it has been reported that during the isopropanol dehydration over sulfated titania, the highest formation of isopropyl ether was found in the catalysts showing the highest acid site density [20]. In Table 1, the catalyst showing the highest selectivity to isopropyl ether is the catalyst with the highest nickel content. To this catalyst corresponds the highest acid sites density (last column). It must be note that, during 5 h on stream, no changes in activity or selectivity were produced. In a large number of papers, it has been reported that the zirconia tetragonal phase is the most active for acid–base reactions [17]. However, in our case we have nickel supported over sulfate zirconia and hence, the acidity of the support was

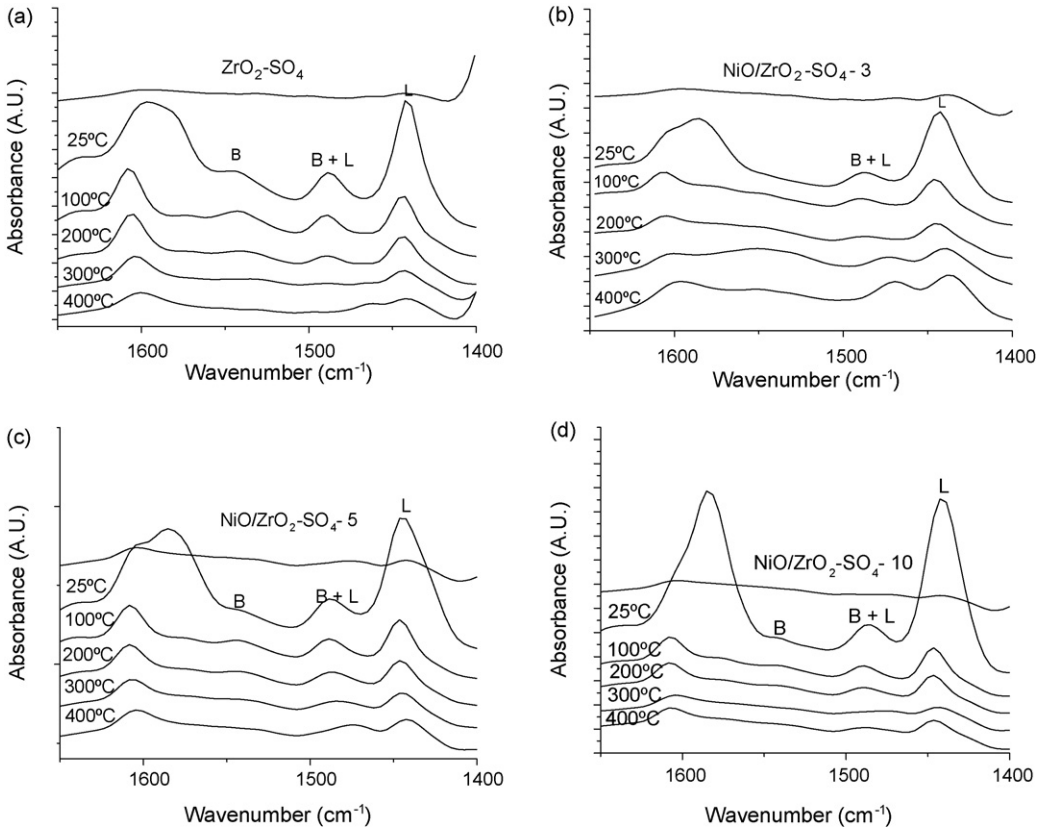

Fig. 2. FTIR-pyridine thermodesorption for NiO/ZrO_2–SO_4-X catalysts.

strongly modified by the nickel content effect. Then, it seems that a crystalline phase effect does not operate in our catalysts.

As mentioned before, the isopropanol dehydration was carried out as a catalytic test in order to determine, in an indirect way, the superficial acidity in our catalysts. The results will be considered to make an interpretation of the behavior of the nickel zirconia sulfated catalysts in the isobutene oligomerization.

4.5. Isobutene oligomerization

The isobutene oligomerization in function of the time on stream is presented in Fig. 4. The catalysts showed conversion values of 20, 29, 33 and 36% for ZrO_2–SO_4, NiO/ZrO_2–SO_4-10, NiO/ZrO_2–SO_4-5 and NiO/ZrO_2–SO_4-3, respectively, after 2 h on stream. The catalysts with the lowest nickel content are the most active. Hence, the activity for the oligomerization reaction follows an inverse order to that observed for the isopropanol dehydration. The oligomerization of butenes is a reaction which depends strongly of the acidity of the catalyst; however, a strong deactivation occurs at the same time. In Fig. 4 it can be seen that, ZrO_2–SO_4 is the catalyst which showed the highest deactivation rate, according to its highest acidity. On the other hand, the NiO/ZrO_2–SO_4 catalysts at 3 and 5 wt% Ni content, showed a large stability, being their activity the highest

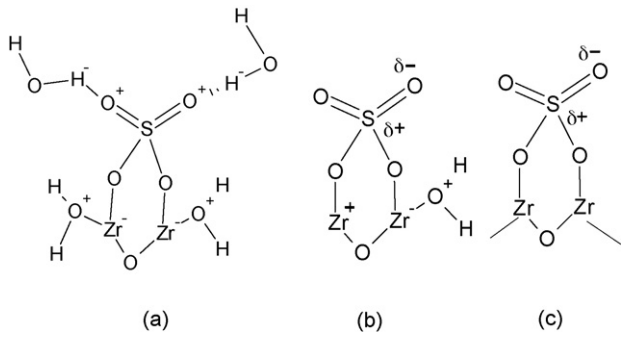

Fig. 3. Modified structures [17] denoting Brönsted (a) and Lewis (b and c) acid sites on ZrO_2–SO_4 catalysts.

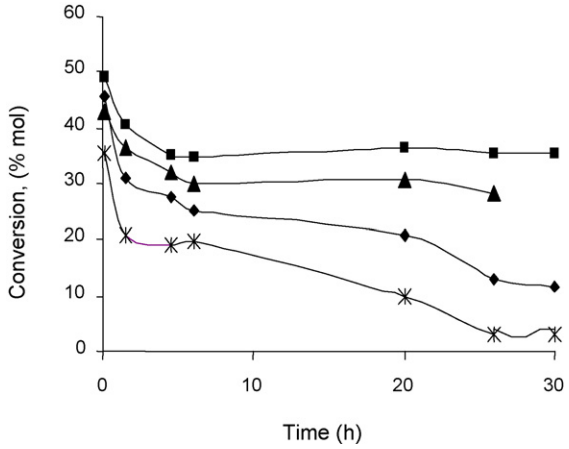

Fig. 4. Conversion of isobutene as function of time for the various catalysts at 28 °C, atmospheric pressure and GHSV = 16 h^{-1}.

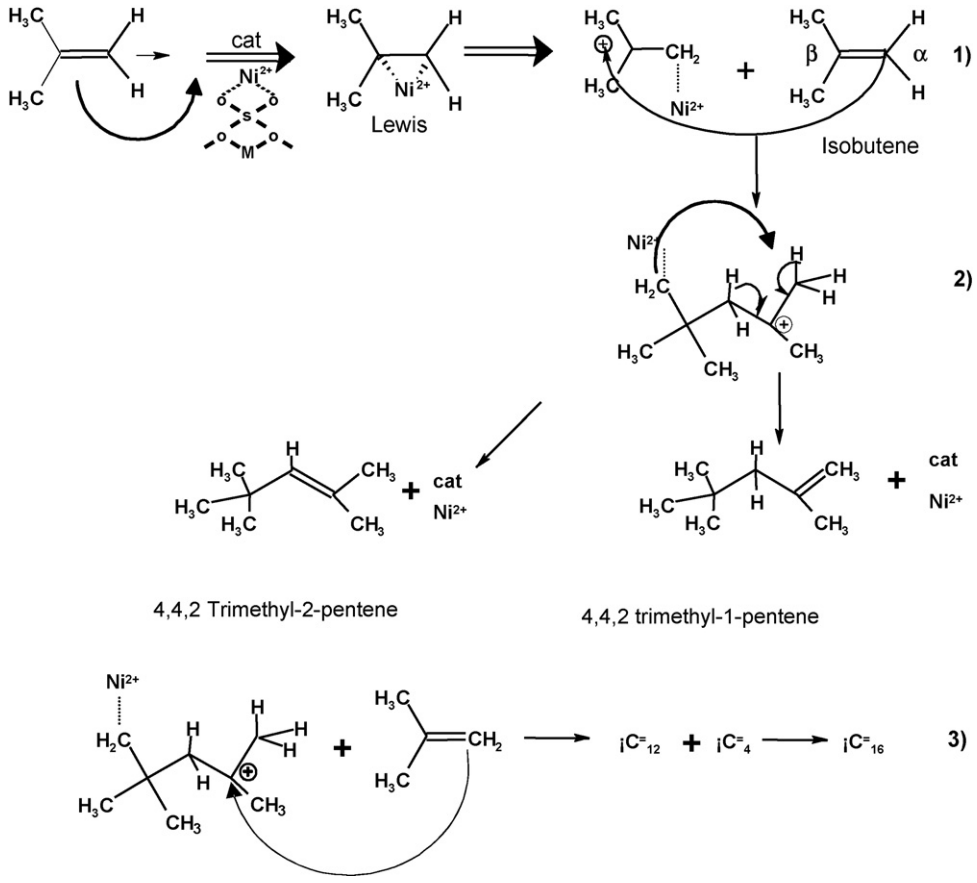

Fig. 5. Oligomerization of isobutene on NiO/ZrO_2–SO_4 catalysts.

of all the samples. The effect of nickel as stabilizer, reported in Ni/zeolites [12–14], is also observed in nickel zirconia sulfated catalysts. For the catalyst with 10 wt% of Ni, the behavior is totally different, because this is the catalyst showing the lowest acidity; however, its deactivation is really notorious.

The role of nickel in dimerization/oligomerization reactions has been related to the presence of Ni^{+2}, which diminishes the deactivation rate by its capacity to coordinate π-allyl electrons of the olefin [21]. As a result, its presence generates a competitive effect with the acid sites, avoiding the oligomerization. This asseveration is true for the catalyst with 3 and 5 wt% Ni; however, in the catalyst with a Ni content of 10 wt%, we can observe that the competitive effect with the acid sites is very important and then, it acts as an inhibitor of the dimerization of isobutene. Nickel can act as an active center for this reaction, as it is illustrated in Fig. 5.

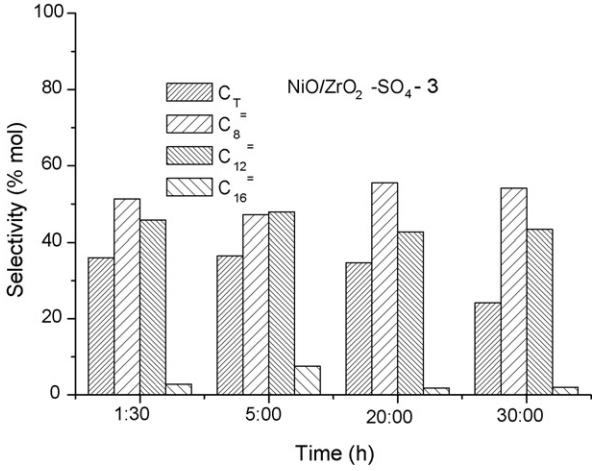

Fig. 6. Selectivity to $C_8^=$, $C_{12}^=$ and $C_{16}^=$ for the oligomerization of isobutene as a function of time for NiO/ZrO_2–SO_4-3 catalyst at 28 °C, atmospheric pressure, GHSV = 16 h^{-1}.

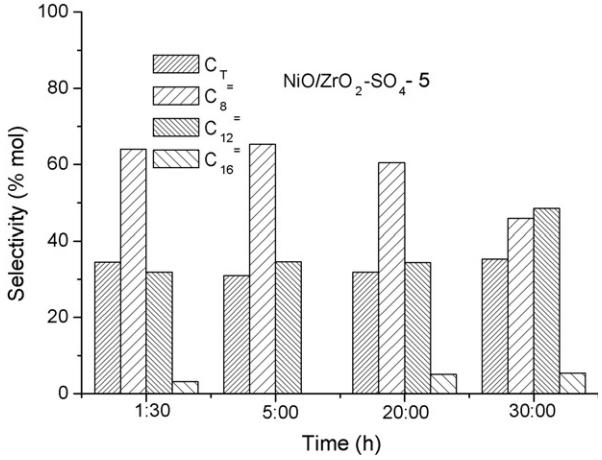

Fig. 7. Selectivity to $C_8^=$, $C_{12}^=$ and $C_{16}^=$ for the oligomerization of isobutene as a function of time for NiO/ZrO_2–SO_4-5 catalyst at 28 °C, atmospheric pressure, GHSV = 16 h^{-1}.

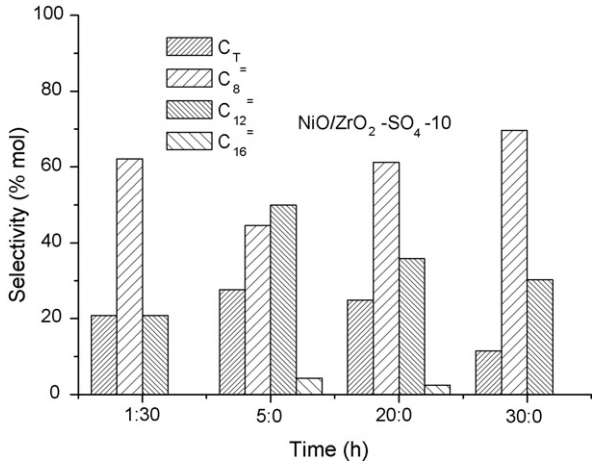

Fig. 8. Selectivity to $C_8^=$, $C_{12}^=$ and $C_{16}^=$ for the oligomerization of isobutene as a function of time for NiO/ZrO_2–SO_4-10 catalyst at 28 °C, atmospheric pressure, GHSV = 16 h^{-1}.

Note that, the catalyst with 5 wt% of Ni is slightly more active than the catalyst with 3 wt% of Ni; thus, there is a maximum in the positive effect of nickel as a stabilizer in the olefin oligomerization reaction.

The selectivity patterns of selectivity to the $C_8^=$, $C_{12}^=$ and $C_{16}^=$ fractions for the various nickel zirconia sulfated catalysts are shown in Figs. 6–8. The catalyst with 3 wt% of Ni showed selectivities in the same order for $C_8^=$ and $C_{12}^=$ fractions. However, for the catalyst with 5 wt% of Ni, the selectivity to the $C_{12}^=$ fraction is notably diminished, showing the stabilizing role of Ni. For the catalyst with 10 wt% of Ni, the selectivity to the $C_8^=$ olefins fraction is the best; nevertheless, this is the catalyst showing the highest deactivation rate. It must be noted that the $C_{16}^=$ olefins fraction was present in the products but only in a minimal percentage (<5%).

5. Conclusions

In the synthesis of nickel zirconia sulfated catalysts, using zirconium alkoxide and nickel sulfate as starting materials, the solids showed high specific surface areas, comprised between 108 and 52 m^2/g. XRD patterns showed the co-existence of tetragonal and monoclinic zirconia in samples annealed at 600 °C; however, a stabilizing effect of the tetragonal zirconia crystalline phase was observed when the content of nickel was of 10 wt%. From FTIR-pyridine thermodesorption, it is showed that Lewis and Brönsted sites are developed in sulfated zirconia catalyst, while in nickel zirconia sulfated catalysts only Lewis acid sites were observed. The amount of pyridine adsorbed determined by FTIR correlated well with the activity for the isopropanol dehydration reaction. The highest activity corresponds to the catalysts showing the strongest acidity (Lewis and Brönsted sites). For the isobutene oligomerization, it is showed the opposite effect: the catalysts with the highest acidity were the less active and those who showed the highest deactivation rate. The role of nickel in dimerization/oligomerization of isobutene has been related to the presence of Ni^{+2}, which diminishes the deactivation rate by its capacity to coordinate π-allyl electrons of the olefins. It is showed that the selectivity to $C_8^=$ and $C_{12}^=$ olefins fractions depends strongly of the nickel content.

Acknowledgement

We acknowledge the support given by the CONACYT.

References

[1] M. Golombok, J. De Bruijn, Ind. Eng. Chem. Res. 39 (2000) 267.
[2] M. Golombok, J. De Bruijn, Appl. Catal. A: Gen. 208 (2001) 47.
[3] M. Golombok, J. De Bruijn, Chem. Eng. Res. Dev. 78 (2000) 145.
[4] M. Marchionna, D. Girolamo, R. Patrini, Catal. Today 65 (2001) 397.
[5] R. Alcántara, E. Alcántara, L. Canoira, M.J. Franco, M. Herrera, A. Navarro, React. Funct. Polym. 45 (2000) 19.
[6] J.H. Gary, G.H. Hadwerk, Petroleum Refining Technology and Economics, 3rd ed., Dekker, New York, 1994.
[7] A. Mantilla, F. Tzompantzi, G. Ferrat, A. López-Ortega, E. Romero, E. Ortiz-Islas, R. Gómez, M. Torres, Catal. Today 107–108 (2005) 707.
[8] A. Mantilla, F. Tzompantzi, G. Ferrat, A. López-Ortega, E. Romero, E. Ortiz-Islas, R. Gómez, M. Torres, CRS chemical industries series 115, in: S.R. Schmidt (Ed.), Catalysis of Organic Reactions, Taylor & Francis Press, Boca Raton, FL, 2007, p. 61.
[9] A. Mantilla, F. Tzompantzi, G. Ferrat, A. López-Ortega, E. Romero, F. Tzompantzi, E. Ortiz-Islas, R. Gómez, M. Torres, Chem. Commun. (2004) 1498.
[10] A. Mantilla, G. Ferrat, A. López-Ortega, E. Romero, F. Tzompantzi, M. Torres, E. Ortiz-Islas, R. Gómez, J. Mol. Catal. A: Chem. 228 (2005) 333.
[11] C.H. Bartholomew, Appl. Catal. A: Gen. 212 (2001) 17.
[12] B. Nkosi, F.T.T. Ng, G.L. Rempel, Appl. Catal. A: Gen. 158 (1997) 225.
[13] B. Nkosi, F.T.T. Ng, G.L. Rempel, Appl. Catal. A: Gen. 161 (1997) 153.
[14] G.G. Podrebarac, F.T.T. Ng, G.L. Rempel, Appl. Catal. A: Gen. 147 (1996) 159.
[15] A.A. Davydov, M. Kantcheva, M.L. Chepotko, Catal. Lett. 85 (2002) 97.
[16] R. Gomez, T. Lopez, E. Ortiz-Islas, J. Navrrete, E. Sanchez, F. Tzompantzi, X. Bokhimi, J. Mol. Catal. A: Chem. 193 (2003) 217.
[17] S. Ben Chaabene, L. Bergaoui, A. Ghorbel, J.F. Lambert, P. Grange, Appl. Catal. A: Gen. 268 (2004) 25–31.
[18] X. Chen, Y. Shen, S.L. Suib, C.L. O'Young, J. Catal. 197 (2001) 292.
[19] A. Gervassini, J. Fenyvesi, A. Auroux, Catal. Lett. 43 (1997) 219.
[20] E. Ortiz-Islas, T. López, J. Navarrete, X. Bokhimi, R. Gómez, J. Mol. Catal. A: Chem. 228 (2005) 333.
[21] J. Heveling, C.P. Nicolaides, M.S. Scurrell, Appl. Catal. A: Gen. 248 (2003) 239.